



HAL
open science

Establishment of a Long-Term Primary Culture of Oyster Hemocytes and Novel Insights About Their Function, Metabolism, and Behavior

Danielle F Mello, Rafael Trevisan, Yasmine Even, Valentin Foulon, Christophe Lambert, Heloisa Gabe, Manon Le Goff, Claudie Quéré, Fernando R Queiroga, Christophe Brigaudeau, et al.

► To cite this version:

Danielle F Mello, Rafael Trevisan, Yasmine Even, Valentin Foulon, Christophe Lambert, et al.. Establishment of a Long-Term Primary Culture of Oyster Hemocytes and Novel Insights About Their Function, Metabolism, and Behavior. 2024. <hal-04884166>

HAL Id: hal-04884166

<https://hal.science/hal-04884166v1>

Preprint submitted on 13 Jan 2025

HAL is a multi-disciplinary open access archive for the deposit and dissemination of scientific research documents, whether they are published or not. The documents may come from teaching and research institutions in France or abroad, or from public or private research centers.

L'archive ouverte pluridisciplinaire HAL, est destinée au dépôt et à la diffusion de documents scientifiques de niveau recherche, publiés ou non, émanant des établissements d'enseignement et de recherche français ou étrangers, des laboratoires publics ou privés.



HAL Authorization

1 Establishment of a long-term primary culture of oyster hemocytes and novel insights 2 about their function, metabolism, and behavior

3 Danielle F. Mello¹; Rafael Trevisan^{1§}; Yasmine Even^{1§}; Valentin Foulon²; Christophe Lambert¹; Heloisa Gabe¹;
4 Manon Le Goff¹; Claudie Quéré¹; Fernando R. Queiroga¹; Christophe Brigaudeau³; Hélène Talarmin⁴; Caroline
5 Montagnani⁵; Guillaume M. Charrière⁵; Delphine Destoumieux-Garzon⁵; Stéphanie Madec^{1*} and Charlotte
6 Corporeau^{1*}

7
8 ¹ Univ Brest, Ifremer, CNRS, IRD, LEMAR, IUEM, F-29280 Plouzane, France.

9 ² ENIB, UMR CNRS 6285 LabSTICC, F-29238, Brest, France.

10 ³ Univ Brest, INSERM, EFS, UMR 1078, GGB, F-29200 Brest, France.

11 ⁴ Univ Brest, ORPHY EA 4324, F-29200 Brest, France.

12 ⁵ IHPE, Univ Montpellier, CNRS, IFREMER, Univ Perpignan Via Domitia, Montpellier, France.

13 * Co-last authors

14 § These authors contributed equally to this work.

15

16 Abstract

17 This study aims to develop a comprehensive and standardized protocol for the primary cell culture of oyster hemocytes
18 and their structural and functional analyses. Hemocytes are crucial for immune defense and overall bivalve health.
19 Current primary culture systems for bivalve hemocytes are limited in duration, making long-term studies challenging.
20 Here, we adopted the approach of utilizing hemolymph plasma as our complete and natural culture medium
21 maintaining live, active, and immunocompetent oyster hemocytes throughout 21 days of culture period. Distinct types
22 of hemocytes are described based on their morphology and function in primary culture. Granulocytes and hyalinocytes
23 displaying various shapes and spreading patterns, in addition to blast-like cells, were cultured for up to 7 days. Between
24 14 and 21 days, blast-like cells and hyalinocytes decreased in number with signs of apoptosis, revealing a
25 subpopulation of hemocytes with a higher resistance for *in vitro* maintenance. Live-cell imaging revealed that the
26 remaining cells were kept alive and active throughout the 21 days of culture. Two primary cell motility behaviors were
27 observed: pseudopod-dependent and lamellipodium-dependent membrane extensions, which are reminiscent of the
28 mesenchymal and amoeboid migration modes, respectively. The proportion of about 40 % of the hemocytes displaying
29 phagocytic activity within fresh hemolymph was maintained throughout the 21-day culture period. However, the
30 phagocytic capacity was higher within phagocytes present after 14 and 21 days of culture. Metabolic assays revealed
31 alterations in reactive oxygen species production and neutral lipid storage, suggesting physiological alterations in
32 response to the culture environment. Our research established a robust protocol for long-term primary cell culture and
33 assessment of bivalve hemocyte health, function, and metabolism. This protocol, potentially applicable to hemocytes
34 of other marine bivalve species, paves the way to enhance our understanding of bivalve immunology and cellular
35 physiology and ecophysiology. This valuable tool can be applicable for future research in marine biology,
36 biotechnology, environmental science, ecotoxicology, and comparative physiology.

37 **Keywords:** Invertebrates; *Crassostrea gigas*; immune cells; live-cell imaging.

38 1. Introduction

39 Hemocytes are specialized cells found in the circulatory system of invertebrates, such as marine bivalves, and play
40 crucial roles in physiology and health. Hemocytes are immune cells acting as the first line of defense against pathogens,
41 parasites, and foreign particles. The most important functions of hemocytes are the detection and engulfment of
42 invading microorganisms through phagocytosis and the production of proteolytic and antimicrobial molecules,
43 effectively neutralizing these threats and preventing infections. Hemocytes are also involved in encapsulation, a
44 mechanism where they surround larger foreign bodies or parasites that cannot be readily phagocytosed. By
45 encapsulating these threats, hemocytes prevent their spread and limit the damage caused to the tissues. Hemocytes also
46 participate in wound healing and tissue repair when a bivalve sustains an injury: they migrate to the site of damage and
47 assist in sealing the wound, facilitating the regeneration of damaged tissues. They also contribute to other physiological
48 processes than immunity, including nutrient transport, maintaining osmotic balance, shell mineralization, and the
49 elimination of metabolic wastes from the hemolymph [1–3].

50 The study of hemocyte biology has emerged as a fundamental aspect of ecotoxicology and ecophysiology research in
51 understanding the resilience and adaptability of marine bivalves in their natural environments and the context of
52 environmental changes. Measuring the functions of hemocytes (*e.g.*, phagocytosis and viability) and their abundance
53 (*e.g.*, number of cells per volume of hemolymph) have long been used as key indicators of the overall health and
54 physiological condition of bivalves [4]. Indeed, changes in hemocyte numbers, morphology, or function may reflect
55 the exposure to pollutants, toxins, or environmental stressors, making them valuable biomarkers for assessing
56 environmental quality and the impact of human activities on marine ecosystems [5–7]. Thus, research focusing on
57 hemocyte biology is crucial for predicting and mitigating the impacts of a diversity of stressors like ocean acidification,
58 pollution, and climate change on bivalve populations. This can support the development of strategies aiming at the
59 conservation and management of bivalve populations and their coastal environments under current and future
60 environmental conditions.

61 The Pacific oyster *Crassostrea gigas* (Thunberg, 1793) is a marine invertebrate that holds a major economic and
62 ecological significance at the global scale. It is one of the most cultivated shellfish around the world and an abundant
63 mollusk species in an increasing number of coastal areas. *C. gigas* is widely used as a sentinel bivalve species for
64 biomonitoring studies in coastal marine environments [8] and to understand the impacts of environmental stressors [9].
65 In such studies, the effects on oyster health are often evaluated by assessing hemocyte parameters *ex vivo* [10–16].
66 However, typically, this approach requires large facilities, expensive experimental conditions, co-maintenance of
67 microalgae cultures for animal feeding, and intensive hemolymph sampling on the days of experimentation.

68 *In vitro* studies provide numerous advantages for biological research. They are potent and valuable tools in marine
69 bivalve research, offering crucial insights into the physiology, health, and responses of these organisms to various
70 environmental stressors [17–21]. *In vitro* cell studies can provide the investigation of precise mechanisms (gene
71 expression, enzyme activities, biomarkers) linked to changes in cell function, morphology, and metabolism, shedding
72 light on how individuals adapt their cellular responses to environmental challenges. Another key advantage lies in the
73 possibility of controlling the microenvironment around cells and providing standardized conditions for such studies.
74 For example, temperature, pH, salinity, and pollutant concentrations can be controlled to study isolated or combined
75 factors or to simulate real-world conditions. This is particularly important for bivalves, who are constantly exposed to
76 a variety of environmental stressors such as temperature, food, and oxygen fluctuations within the intertidal zone, as
77 well as pathogens and pollutants [22–25]. Additionally, *in vitro* studies reduce ethical concerns associated with *in vivo*
78 experiments, as they minimize the number of animals needed for large-scale experimentation. *In vivo* studies not only
79 require a greater number of animals to be sacrificed but also, in the case of waterborne pollutant exposures, they
80 generate significantly larger amounts of chemical waste. Nonetheless, maintaining viable and functional bivalve
81 hemocytes under *in vitro* conditions for periods longer than 2–4 days has been a major challenge [26]. In this study,
82 we developed a standardized protocol to maintain primary cell cultures of *C. gigas* hemocytes viable and in an active
83 immunological state for at least 21 days. Additionally, we provide a panel of structural, functional, and metabolic
84 parameters that can be used as indicators of hemocyte physiological state. Therefore, this study provides a promising
85 *in vitro* cellular platform paving the way for in-depth investigation of hemocyte functions *in vitro* that supplement *in*
86 *vivo* research on cellular biology, immunology, ecophysiology, and ecotoxicology of marine bivalves.

87 2. Methods

88 2.1 Animals

89 Hatchery-produced adult *C. gigas* (triploid, size n^o2 – 86-110 g of whole-body weight) were obtained from an oyster
90 farm (Beg Ar Vil) located at the Aber Benoit (France), an area considered to have a low anthropogenic impact [27].
91 The main reasons why choosing triploid oysters over the naturally occurring diploid ones are their easy access through
92 the aquaculture industry, the possibility of obtaining hemolymph without contamination by gametes all year long, and
93 the absence of major metabolic changes induced by reproductive maturation. Oysters were conditioned from 48 h up
94 to 4 weeks before cell sampling. They were maintained either in natural seawater with natural food source at Ifremer's
95 experimental site (Ste Anne, Plouzané, France) or under controlled conditions with seawater temperature at 16±1.5 °C,
96 constant aeration, water flow, and daily feeding by a commercial phytoplankton diet (0.5 mL per animal; SA Live
97 Marine Phytoplankton®, Premium Blend) in the laboratory (Plouzané, France).

98 2.2 Hemolymph collection

99 Hemolymph was collected by performing a small notch in the shell immediately before sampling. A cold 1 mL syringe
100 coupled with a 23G x 1" needle was injected into the adductor muscle, and hemolymph was gently withdrawn, avoiding
101 bubbles and seawater contamination. A drop of each hemolymph sample collected was used to inspect hemolymph
102 quality under a light microscope using both 4× and 10× objectives. Only samples containing zero visualization of
103 contaminants (e.g., tissue and cellular debris and visible microorganisms: bacteria, protozoa, and microalgae) and no
104 excessive hemocyte aggregation were used. Hemolymph samples that passed this rigorous quality check were pooled
105 in 15 mL centrifuge tubes maintained on ice. Hemolymph collection usually lasted about 1 h but depending on the
106 volume needed and easiness of collection, collection time varied between 1-3 h. Both the rigorous quality check of
107 each hemolymph extraction and the limited time on ice (up to 3 h) were critical factors for the success of the primary
108 cultures. The hemolymph sampling for the optimization experiments was conducted between February 2022 and
109 September 2022. Samplings for the three independent 21-day experiments were conducted in November 2022
110 (autumn), April 2023 (spring) and May 2023 (spring). In the first experiment, two independent pools of hemolymph
111 were analyzed (N=2), while in the second and third experiments, five independent pools of hemolymph were analyzed
112 (N=5 for each). Each hemolymph pool consisted of samples from 2-6 oysters.

113 2.3 Primary hemocyte cultures

114 The first step in preparing the primary hemocyte cultures was to determine the concentration of hemocytes in
115 hemolymph pools. For this, 50 µL of well-homogenized hemolymph pool was mixed with 50 µL of filtered sterile
116 seawater (FSSW; 0.22 µm polyethersulfone -PES- syringe filter) containing 3.9 % formaldehyde to avoid cell
117 clumping and adherence to the counting chamber, which are detrimental factors for accurate counting). Then 10 µL of
118 the fixed hemolymph was added to the counting slides adapted to the EVE™ Automatic Cell Counter. Once the cell
119 concentration was determined, whole hemolymph pool samples containing 500.000 or 80.000 cells were seeded into
120 each well of 24 or 96-well plates (~250 000 cells/cm²), respectively. Plates were pre-coated with poly-D-lysine either
121 from the manufacturer or at the laboratory following the manufacturer's protocol (Gibco™, ThermoFisher Scientific,
122 A3890401; for microplate references, see Supp. Tab. 1). The microplates containing the freshly seeded cells were then
123 incubated for at least 1 h (up to 3 h) at 16±1 °C for adherence using a standard cooling incubator (Mettler IPP55;
124 which uses ambient air, i.e., no O₂ or CO₂ control). The supernatant was then gently completely removed and replaced
125 with the hemocyte culture media. As a first step, different media and other culture conditions were tested (Supp. Tab.
126 2). The quality of hemocyte primary cultures within the different test conditions was screened by microscopic
127 examination daily, observing cell morphology and adherence, and possible signs of contamination (see Results section
128 for a detailed description of our definition of cultures presenting good quality conditions). The cell culture medium
129 that provided optimum cell culture conditions was composed of filtered-sterile oyster plasma (FSOP) containing
130 penicillin (+P) 100 U/ml and streptomycin (+S) 100 µg/ml (Gibco™, ThermoFisher Scientific, 15140148). The FSOP
131 medium predominantly consisted of two pools of whole hemolymph samples from about 100 oysters (each collected
132 at two different periods, September 2022 and March 2023), which were filtered (0.22 µm PES syringe filter), split into
133 aliquots, and stored without antibiotics at -80 °C until use. A minor part of fresh FSOP was eventually used at the start

134 of the cultures, whereas FSOP from the -80 °C bank was always used for complete medium renewal every 7 days. A
135 final volume of 500 µL or 100 µL of the cell culture medium FSOP+P/S was used for the 24 or 96-well plates,
136 respectively.

137 **2.4 Characterization of cell morphotypes and behavior**

138 We combined both May-Grünwald Giemsa staining with live-cell imaging to characterize the cells present in our oyster
139 primary hemocyte cultures over time. All assays described in this section were optimized to be conducted in cells
140 cultured in 96-well microplates.

141 For the May-Grünwald Giemsa (MGG; RAL Diagnostics, 320070) staining, microplates were centrifuged (1000 ×g,
142 5 min, 16 °C), the supernatant was carefully removed, replaced with 100 µL of May-Grünwald and incubated for 3
143 min at room temperature. Then, 200 µL of distilled H₂O was added and samples were incubated for an extra 1 min.
144 The supernatant was then removed, cells were rinsed once with 200 µL of distilled H₂O, and incubated with 100 µL
145 of Giemsa R solution for 10 min. Finally, the supernatant was removed, and cells were rinsed with 200 µL of distilled
146 H₂O. Plates were left to dry, and just before the microscope visualization, a drop of microscopy immersion oil was
147 added to each well to improve cell visualization. Images were recorded using an inverted microscope (Zeiss AXIO
148 Observer Z1) coupled with a color camera system (Canon EOS 700D).

149 Live unstained cells were imaged through phase-contrast microscopy (EVOS XL Core Imaging System, ThermoFisher
150 Scientific) or Confocal Laser Scanning Microscopy (Zeiss LSM780, Carl Zeiss) using the transmitted-light channel
151 equipped with a photomultiplier (TPMT). Phase-contrast and transmitted-light TPMT images were taken every 10s or
152 3s, using ×10 or ×40 air objectives, respectively.

153 The phagocytic behavior of hemocytes in primary cultures was performed by time-lapse imaging of cells incubated
154 with Fluoresbrite® YG Microspheres beads (2 µm, Polysciences Inc.). The beads were added to the primary cultures
155 at a final concentration of 0.005 %, and cultures were incubated for 4 hours at 16±1 °C before imaging. Image
156 acquisition was performed every 10 s for 3 min at room temperature (20±1 °C) using the transmitted-light channel of
157 the Zeiss AXIO Observer Z1 coupled with the Canon EOS 700D color camera system.

158 Time-lapse videos were created with the MakeAVI software using 5 frames per second (each second of the video
159 corresponds to 50 s in real-time), except for the videos using confocal transmitted-light TPMT images, which were
160 created with the ZEN 2012 software (Carl Zeiss) using 10 frames per second (each second of the video corresponds to
161 30 s in real-time).

162 **2.6 Cellular physiological parameters**

163 Cellular parameters involving size, complexity, viability, immune function, and metabolism were analyzed on
164 hemocytes maintained in primary cultures over time. Assays were performed through flow cytometry (cell viability,
165 ROS production, phagocytosis, and mitochondrial and neutral lipid contents) or by multimode plate readers (ATP
166 content and NADH production) as described below. For these assays, the start of each primary cell culture was
167 staggered, meaning that cells were seeded 21, 14, and 7 days before the day of the analysis and compared to fresh
168 hemolymph samples (Day 0). The assays were thus performed on the same day so that all cell culture time points could
169 be more readily comparable. Therefore, it is important to highlight that each time-point of the cell-based assays
170 corresponded to cultures obtained from different hemolymph pools (thus different oysters).

171 Flow cytometry analyses were performed from primary hemocyte cultures maintained in 24-well plates (Supp. Tab.
172 1). Cells were recovered from the wells by gentle repetitive pipetting of the cell culture medium within each well and
173 transferred to centrifuge microtubes on ice. The fresh hemolymph (Day 0, used as control) was collected and
174 maintained in centrifuge microtubes on ice without deposition into the microplate to avoid cell loss (as within the first
175 hours of cell culture, most hemocyte types tend to be more adherent to the bottom of the well and cannot be easily
176 detached). Flow cytometry assays were performed by transferring 50 µL of cells into flow cytometer tubes containing
177 150 µL of FSSW containing different fluorophores. Cell viability was measured by incubation with 10 µg/mL of
178 propidium iodide (Sigma, France) and 1X SYBR Green I (10,000X stock; Sigma, France) for 30 min, at 18 °C, in the
179 dark [28]. Cell size and complexity were quantified using the same samples stained for cell viability through

180 measurements obtained by the side scatter (SSC), representing the granularity or internal complexity of particles, and
181 the forward scatter (FSC), estimating the size of particles. SYBR Green I-stained hemocytes could be distinguished
182 from other hemolymph particles by gating and differentiating them using a density plot visualization of SSC vs. FL1,
183 displayed on a log scale [28]. For the quantification of ROS production, incubation was performed with 10 μ M
184 dichlorodihydrofluorescein diacetate (DCFH-DA; Sigma, France) for 60 min, at 18 °C, in the dark [29]. Hemocyte
185 phagocytosis was measured using the final concentration of Fluoresbrite® YG Microspheres beads at 0.005 % (2 μ m,
186 Polysciences Inc., France) and incubation was performed for 120 min, at 18 °C, in the dark. The percentages of active
187 phagocytes were defined as the percentage of cells that ingested three or more beads [30]. Mitochondrial content,
188 mitochondrial ROS production, and neutral lipid content were measured according to the manufacturer's protocols.
189 Mitochondrial content was assessed by incubating cells with a 1/1,000 dilution of MITO-ID® Green (Enzo Life
190 Sciences) for 1 h at 18 °C, in the dark. Mitochondrial ROS production was quantified using 5 μ M MitoSOX Red
191 (Thermo Fisher Scientific) and a 30 min incubation period at 18 °C, in the dark. Neutral lipids content was measured
192 by incubating cells with 10 μ M of BODIPY™ 493/503 (Thermo Fisher Scientific) for 15 min at 18 °C, in the dark.
193 Cell viability, ROS production, and phagocytosis analyses were performed on a BD FACSVerse™ flow cytometer
194 (BD Biosciences, San Jose, CA, USA). Mitochondrial content and ROS production and neutral lipid content analyses
195 were performed on a Guava® easyCyte HT System (Luminex, Merck Millipore).

196 ATP production was measured in primary hemocyte cultures maintained in 96-well plates (Supp. Tab. 1) using the kit
197 CellTiter-Glo™ 3D (Promega, G9681), following the manufacturer's protocol with some minor modifications. On the
198 day of the assay, plates were centrifuged (1,000 \times g, 5 min, 16 °C), and the supernatant was carefully removed and
199 replaced with 50 μ L of FSSW plus 50 μ L of the ATP kit reagent. Plates were submitted to linear shaking for 2 min,
200 then samples were transferred to opaque white 96-well plates (Supp. Tab. 1), incubated for 10 min at room temperature,
201 in the dark, and luminescence was recorded using the EnSpire® Multimode Plate Reader (PerkinElmer©). ATP
202 absolute values were calculated based on ATP standard curves (0, 1, 10, 100, 625, 1250, 2500 nM) performed on the
203 same day and plate with the samples.

204 2.7 Statistical Analyses

205 Statistical analyses of the cellular parameter results were performed using the one-way analysis of variance followed
206 by Tuckey's post hoc test. Results were considered significant at $p < 0.05$. All experiments were repeated three times,
207 except for the neutral lipid content and mitochondrial ROS production, which were repeated twice.

208 3. Results

209 3.1 Filtered sterile oyster plasma allows 21 days of robust maintenance of oyster hemocytes *in vitro*

210 Several cell culture conditions were tested to achieve an optimal condition for the *in vitro* maintenance of oyster
211 hemocytes. The conditions included different cell culture media (Supp. Tab. 2), temperatures (20 and 16°C), and plate
212 surfaces (with or without poly-D-lysine coating). The quality of the cultures was first monitored through visual
213 microscopy inspection. Quality criteria included the presence or absence of bacterial and protozoa contamination, and
214 overall cell morphology, diversity, and adherence. Culture contamination events were rare (about 1 in every 10
215 cultures) due to our strict quality control check during hemolymph collection (see Section 2.3 for details) and were
216 mainly due to protozoa when occurred. The culture was considered healthy and not under significant stress when the
217 overall morphology of cells resembled Day 0 primary cultures. Day 0 cultures were characterized by the presence of
218 a mixed population (which will be described in further detail in Section 3.2), with a similar proportion of strongly
219 adhered morphotypes and partially adhered and highly refringent cell morphotypes (Fig. 1). At first, all cell culture
220 media tested contained Leibovitz's L-15 medium in different concentrations (Supp. Tab. 2). These media were tested
221 with or without the

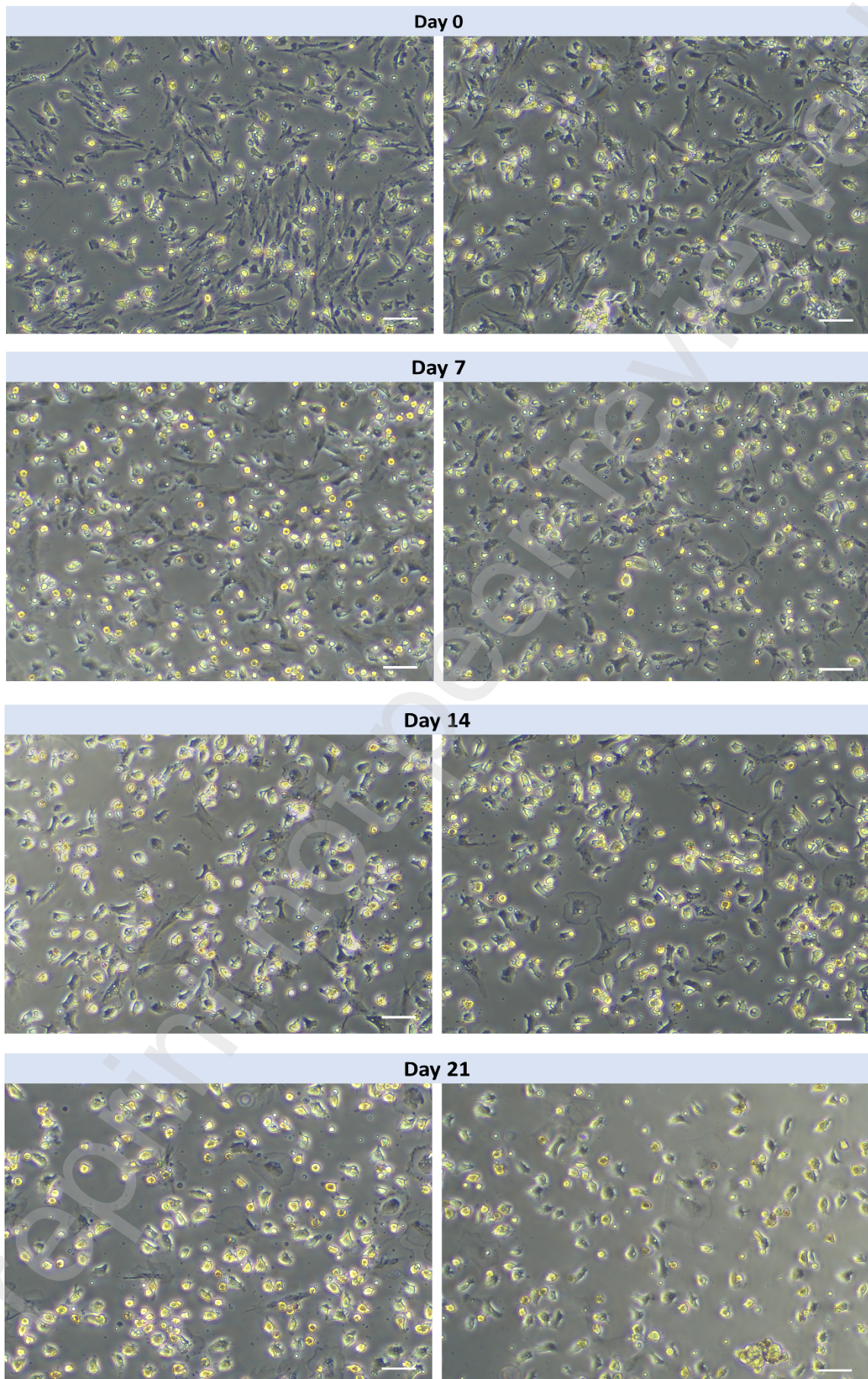


Figure 1. Primary cultures of oyster *Crassostrea gigas* hemocytes throughout 21 days. Cells (500,000/well) were cultivated with filtered-sterile oyster's blood plasma containing antibiotics (FSOP+PS) in 24-well plates coated with poly-D-lysine. The two images from each day correspond to independent cultures. Bar = 50 μ m.

223 addition of fetal bovine serum and with or without the addition of oyster *C. gigas* cell-free hemolymph (filtered sterile
224 oyster plasma or FSOP). All media formulations which were based predominantly on the synthetic Leibovitz's L-15
225 medium were not successful in maintaining healthy oyster hemocyte primary cultures for periods longer than 2 days,
226 as indicated by a predominance of detached round cells, with several cells presenting loss of refringence, and cell
227 aggregates (Supp. Fig. 1). Whereas the addition of 50 % of FSOP within the different media formulations always
228 improved the quality of the cell culture condition by maintaining cell diversity and adhesion (Supp. Fig. 1). This led
229 us to test 100 % FSOP with antibiotics (FSOP+PS) as a culture medium (see Section 2.3 for details). Indeed, cell
230 culture quality improved significantly at this condition, which was further improved by culturing cells using poly-D-
231 lysine as a surface coating.

232 Thus, by cultivating oyster hemocytes within a natural culture medium such as the FSOP combined with low
233 temperatures (~16°C), surface coating (poly-D-lysine), and antibiotics to prevent bacterial contamination, we were
234 able to maintain primary cultures for at least 21 days (Fig. 1). Some culture replicates were able to survive over this
235 period (some lasted over 2 months), but the possibility of obtaining this longer durability was somewhat variable.

236 **3.2 Overall hemocyte diversity and morphology are maintained during the first week of culture**

237 The FSOP+PS medium allowed the maintenance of the same diversity of cell morphotypes as in Day 0 for about 7
238 days of culture (Figs. 1 and 2). During this first week, six major hemocyte morphotypes were identified derived from
239 the three commonly described hemocyte subpopulations: granulocytes, hyalinocytes, and blast-like cells (Fig. 2). Three
240 different cell morphotypes were identified among granulocytes: two presenting high and one presenting low spreading.
241 Granulocytes with low spreading (Fig. 2A) usually displayed a round or dendritic-like shape (Fig. 2A). Granulocytes
242 with high spreading presented either a semi-circular shape (half-moon) (Fig. 2B) or a macrophage-like shape (similar
243 to a fried-egg shape) (Fig. 2C). Among hyalinocytes, we also identified three different cell morphotypes: again, two
244 with high and one with low spreading. Similarly to the granulocytes, hyalinocytes with low spreading also presented
245 a round or dendritic-like shape (Fig. 2D). Hyalinocytes with high cellular spreading were represented by small cells
246 with irregular or half-moon shape (Fig. 2E) or very large cells with elongated (fibroblast-like) or irregular shape (Fig.
247 2F). Finally, blast-like cell morphotypes exhibiting the characteristic high nucleus/cytoplasm ratio and small size were
248 also present (Fig. 2G).

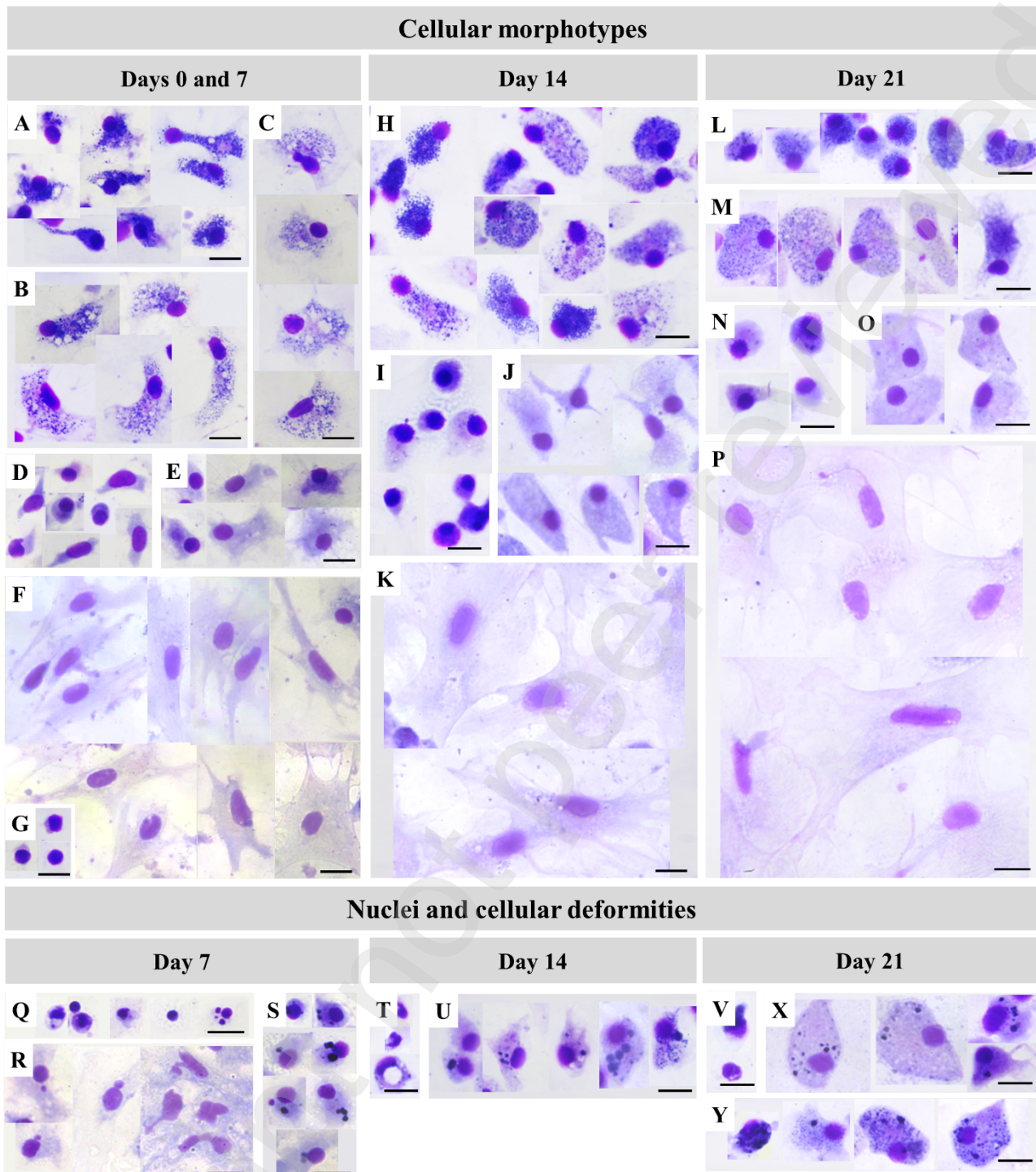
249 **3.3 Notable morphological and cell diversity changes are observed in cells maintained after two weeks of culture**

250 Between 14 days and 21 days of culture, all three commonly described hemocyte subpopulations were represented;
251 however, the blast-like cells and large highly spread hyalinocytes (fibroblast-like cells) were usually less present (Fig.
252 1). When present, the large highly-spread hyalinocytes seemed larger and mostly of irregular shape (Fig. 2K and 2P).
253 Moreover, from 14 to 21 days, the larger granulocytes presented mostly round or oval shape (Figs. 2H and 2M). Also,
254 larger hyalinocytes with round or oval shapes were identified on days 14 and 21 (Figs. 2J and 2O), which were not
255 seen in cultures within the first week.

256 **3.4 Granulocytes are the most prevalent subpopulation at later stages of culture**

257 Overall, it was noticeable by eye a decrease in cell density throughout the culture and a predominance of granulocytes
258 at day 21 (Fig. 1). Such cell loss was correlated with signs of apoptosis, which could be identified by the MGG staining
259 (Fig. 2; bottom panel). Cells presenting the typical signs of apoptosis such as nuclear condensation, loss of cell volume,
260 and nuclear fragmentation were mostly observed on day 7 (Fig. 2Q). Such signs were also seen on days 14 and 21
261 (Figs. 2T and 2V), however with a lower frequency. Other nuclear abnormalities were also mostly observed at day 7,
262 such as micronuclei and blebbing or amorphous nuclei, which were mainly seen among the large and highly spread
263 hyalinocytes (Fig. 2R). In all days of culture (except on day 0), highly pigmented granules were observed within cells
264 presenting normal nucleus morphology, suggesting that these cells had performed the phagocytosis of apoptotic
265 corpses (Figs. 2S, 2U, 2X, and 2Y). Interestingly, cells presenting highly pigmented granules were predominantly
266 hyalinocytes and more frequently seen in cultures from day 7 (Figs. 2S,

267

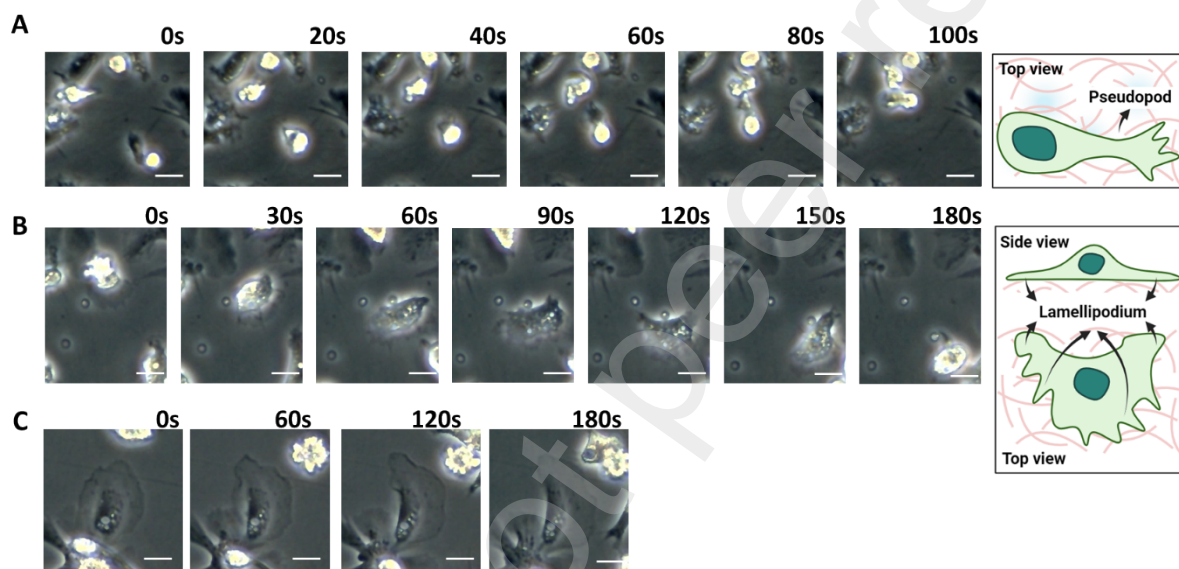


268 *Figure 2.* Morphotypes (top panel) and deformities (bottom panel) of *Crassostrea gigas* hemocytes in primary culture over time. Cells
 269 were cultivated with filtered-sterile oyster's blood plasma with antibiotics (FSOP+PS) in 96-well plates (μ Clear bottom) coated with
 270 poly-D-lysine and colored with May-Grünwald Giemsa. **Morphotypes at days 0 and 7:** (A) small granulocytes with round or dendritic-
 271 like shape; (B) large granulocytes with a semi-circular or half-moon shape; (C) large granulocytes with a macrophage-like or fried-egg
 272 shape; (D) small hyalinocytes with round shape; (E) small hyalinocytes with irregular or half-moon shape; (F) large hyalinocytes with
 273 fibroblast-like or irregular shape; (G) blast-like cells with high nucleus/cytoplasm ratio and small size. **Morphotypes at day 14:** (H)
 274 granulocytes with mostly round or oval shape; (I) small hyalinocytes with mostly round shape; (J) hyalinocytes with oval or dendritic-
 275 like shape; (K) large hyalinocytes with fibroblast-like or irregular shape. **Morphotypes at day 21:** granulocytes with mostly round or
 276 oval shape presenting two different size categories overall: small (L) and large (M); (N) small hyalinocytes with mostly round shape;
 277 (O) larger hyalinocytes with oval shape; (P) large hyalinocytes with mostly irregular shape. **Nuclei and cellular deformities at days**
 278 **7, 14, and 21:** (Q, T, and V) cells presenting the typical signs of apoptosis such as nuclear condensation, loss of cell volume, and/or
 279 nuclear fragmentation; (R) nuclear abnormalities on day 7 cultures such as micronuclei and blebbing or amorphous nuclei; (S, U, X,
 280 and Y) highly pigmented granules within cells presenting normal nucleus morphology, suggesting phagocytosis of apoptotic corpses.
 281 Bar = 10 μ m for all images.

282 2U, and 2X). Nonetheless, these highly pigmented granules were also detected within granulocytes at day 21 (Fig.
283 5Y). The enrichment of granulocytes was further corroborated by the flow cytometry analyses which are described
284 below in section 3.6.

285 3.5 Resistant hemocyte subpopulations are still active and immunocompetent

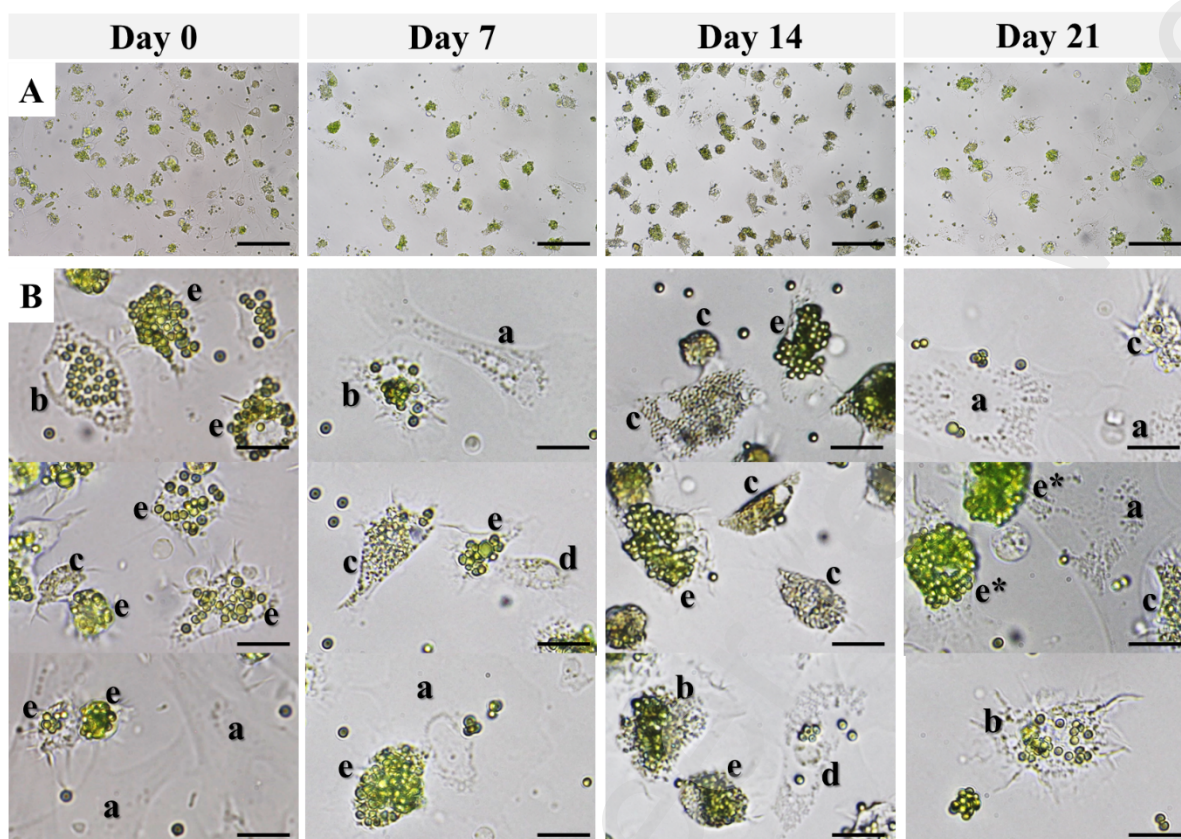
286 Despite the signs described above suggesting cell death, live-cell imaging revealed that most cells from all days of
287 culture were alive as demonstrated by their active motility (see supplementary video files 1-12). We distinguish two
288 main cell movement strategies employed by the hemocytes in culture: movement through pseudopod formation, also
289 known as “mesenchymal migration mode” (Fig. 3A; supplementary video file 13), and movement through
290 lamellipodium formation, also known as “amoeboid migration mode” (Fig. 3B; supplementary video file 14). By
291 comparing the morphotypes seen through the MGG staining images and the ones observed through the time-lapse
292 videos, we suggest that cells displaying a half-moon shape can represent a movement state of the round or dendritic-
293 like morphotypes (Fig. 3B) and of the fried-egg shape morphotype (Fig. 3C). The large highly spread hyalinocytes
294 (fibroblast-like; Fig. 2F) and granulocytes (fried-egg shape) displayed cell membrane expansion and retraction (Fig.
295 3C), however, the cells did not display mobility.



296

297 *Figure 3.* Cell movement behavior of *Crassostrea gigas* hemocytes in primary cultures. Cells were cultivated with filtered-sterile oyster’s blood
298 plasma with antibiotics (FSOP+PS) in 96-well plates (μ Clear bottom) coated with poly-D-lysine. Live-cell imaging revealed two main cell
299 movement strategies employed by the hemocytes in culture: movement through pseudopod or lobopodian formation (A), and movement through
300 lamellipodium formation (B). (C) Cell transitioning from a fried egg shape to a half-moon shape through cell membrane expansion and retraction,
301 but that do not display mobility.

302 To assess if the cell mobility observed in the primary cultures over time could also be associated with immune function,
303 we performed live-cell imaging of the hemocytes in culture in the presence of polystyrene microbeads to observe their
304 phagocytic activity. Cells capable of engulfing the microbeads were observed in all days of culture (Fig. 4).
305 Observation of the time-lapse images revealed distinct phagocytic behaviors for the different cell morphotypes.
306 Overall, three main observations were established: (i) highly spread fibroblast-like cells do not display phagocytic
307 behavior (Fig. 4B, a); (ii) not all highly mobile cells present phagocytosis behavior as some highly mobile cells with
308 (Fig. 4B, c) or without (Fig. 4B, d) granules did not display phagocytic behavior (supplementary video file 15 and 16,
309 respectively); and, finally, (iii) phagocytosis behavior can also be performed by cells presenting none or low motility
310 in culture, such as the highly spread macrophage-like (fried-egg like) cells (Fig. 4B, b; supplementary video 17). We
311 also observed that day 21 cultures seemed to present cells capable of engulfing more microbeads (Fig. 4B-e*) than
312 most phagocytes observed in the other days of culture (Fig. 4B-e).

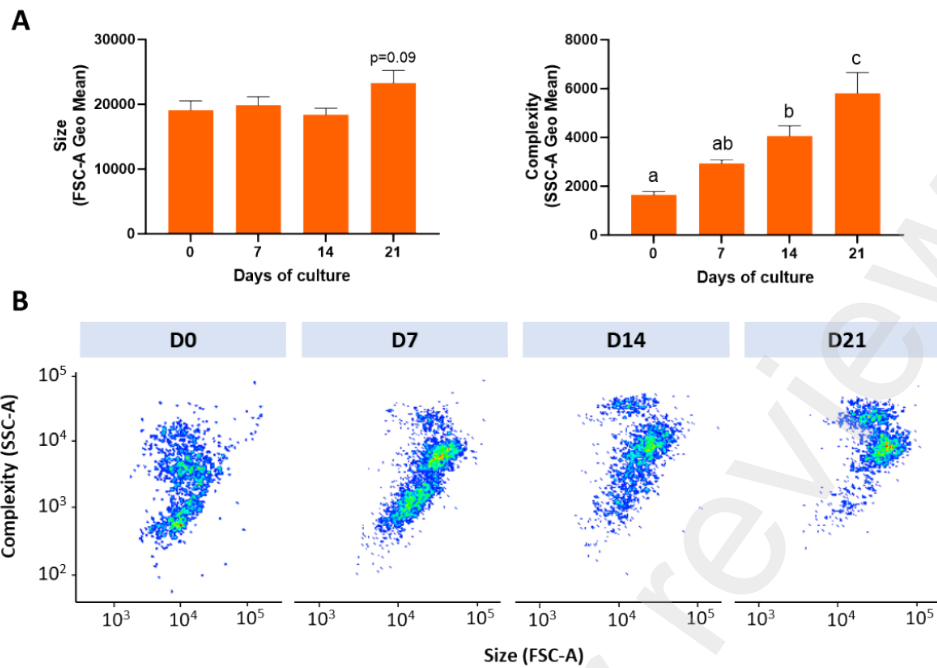


314 *Figure 4.* Phagocytic behavior of *Crassostrea gigas* hemocytes in primary culture over time. Cells were cultivated with filtered-sterile oyster's
 315 blood plasma with antibiotics (FSOP+PS) in 96-well plates (μ Clear bottom) coated with poly-D-lysine and incubated with microsphere beads (2
 316 μ m) for 4 hours at 16 ± 1 °C before imaging. Cells capable of engulfing the microbeads were observed in all days of culture (A). The detailed (B)
 317 observation of images combined with the time-lapse videos revealed distinct phagocytic behaviors of the different cell morphotypes: highly
 318 spread fibroblast-like cells without phagocytic behavior (a); (ii) highly spread macrophage-like (fried-egg) cells which did not display mobility
 319 with phagocytosis behavior (b); highly mobile cells with (c) or without (d) granules without phagocytosis behavior; highly mobile cells capable
 320 of concentrating a great number of beads (e), and possibly an even greater amount within the day 21 cultures (e*). Bar = 10 μ m.

321 In summary, the different morphological and behavioral analyses performed through microscopy imaging revealed
 322 the maintenance of live, active, and immunocompetent cells throughout the 21 days of culture. The cultures evolved
 323 to display fewer hemoblasts and fibroblast-like cells, which possibly died through apoptosis (Fig. 2). Older cultures
 324 seemed to display larger cells overall and present phagocytes with a higher phagocytic capacity.

325 3.6 Maintenance of live and immunocompetent hemocytes with higher complexity

326 We proceeded to flow cytometry analyses to further confirm the live-cell imaging findings and, more precisely,
 327 quantify changes in cell viability, size, and phagocytic capacity of the hemocytes in primary cultures over time.



328
 329 *Figure 5.* Flow cytometry analyses of the size and complexity of oyster *Crassostrea gigas* hemocytes in primary culture over time. Cells
 330 (500,000/well) were cultivated with filtered-sterile oyster's blood plasma containing antibiotics (FSOP+PS) in 24-well plates coated with poly-
 331 D-lysine. (A) Geometric means of cell size and complexity; and (B) representative forward scatter (FSC-A; cell size) vs side scatter (SSC-A;
 332 cell complexity) dot plots, showing the cell distribution within the primary cultures throughout time as compared to control (Day 0, cells
 333 freshly collected). Bars represent means \pm standard deviation. Different letters mean significant differences between groups. Results were
 334 considered significantly different when $p < 0.05$.

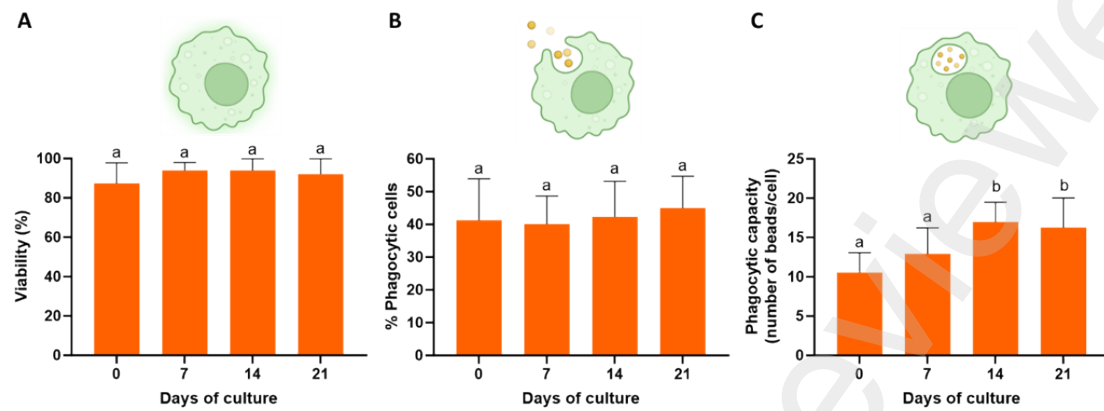
335 Our results reveal that although the mean size of all cells present in the cultures from each day did not significantly
 336 vary, there was a marginally significant increase in size at day 21 and a time-dependent increase in the mean cellular
 337 complexity (Fig. 5A). Such differences were evident through the visualization of forward scatter (cell size) vs side
 338 scatter (cell complexity) dot plots, showing the cell distribution within culture from each culture period (Fig. 5B and
 339 Supp. Figs. 2-5). Classic gating of oyster hemocyte subpopulations, as generally performed in studies using fresh
 340 hemolymph, does not seem the most appropriate to be applied in this study because of the obvious evolution of cell
 341 morphology over time. This makes it difficult to determine which events correspond to hyalinocytes or granulocytes,
 342 for example. Nonetheless, we applied such gating analyses, which revealed a tendency to a decrease in the
 343 proportion of blast-like cells on days 14 and 21 (Supp. Fig. 2). However, no significant changes were detected in the
 344 proportion of "hyalinocytes" and "granulocytes" (Supp. Fig. 2).

345 It is important to note that highly adherent hyalinocytes could not be recovered from wells for the flow cytometry
 346 analyses, as we did not apply any trypsin treatment. This was a choice to avoid cell damage and dysfunction, as we
 347 used such samples for further immunocompetence and metabolic analyses. Thus, even though this approach might
 348 have introduced a bias toward the real proportion of granulocytes in the culture over time, it is evident through whole
 349 primary culture images (Fig. 1) and videos (supplementary video files 1-12) that such highly adherent hyalinocytes
 350 were much less present in cultures after 14 days. This is also evident through images taken after cells were harvested
 351 for the flow cytometry analyses (Supp. Fig. 6).

352 Further flow cytometry analyses were performed to gain quantitative information on hemocyte viability and immune
 353 function. This was done in primary cell cultures from day 0 to 21 days, using propidium iodide staining to measure
 354 cellular membrane integrity and fluorescent microbeads to measure phagocytosis. Despite the decrease in cell
 355 number over time, as discussed above, the remaining cells presented a constant percentage of viable cells from day 0
 356 (fresh, non-plated hemolymph samples) until day 21 (Fig. 6A). Most importantly, these cells kept their
 357 immunocompetence, as demonstrated by the phagocytosis assay (Fig. 6B and C). Interestingly, while the percentage
 358 of phagocytic cells did not change over time (Fig. 6B), the number of microbeads each cell was able to engulf

359 (phagocytic capacity) was higher after 14 and 21 days of culture (Fig. 6C), corroborating the results from the
360 microscopy images (Fig. 4).

361



362

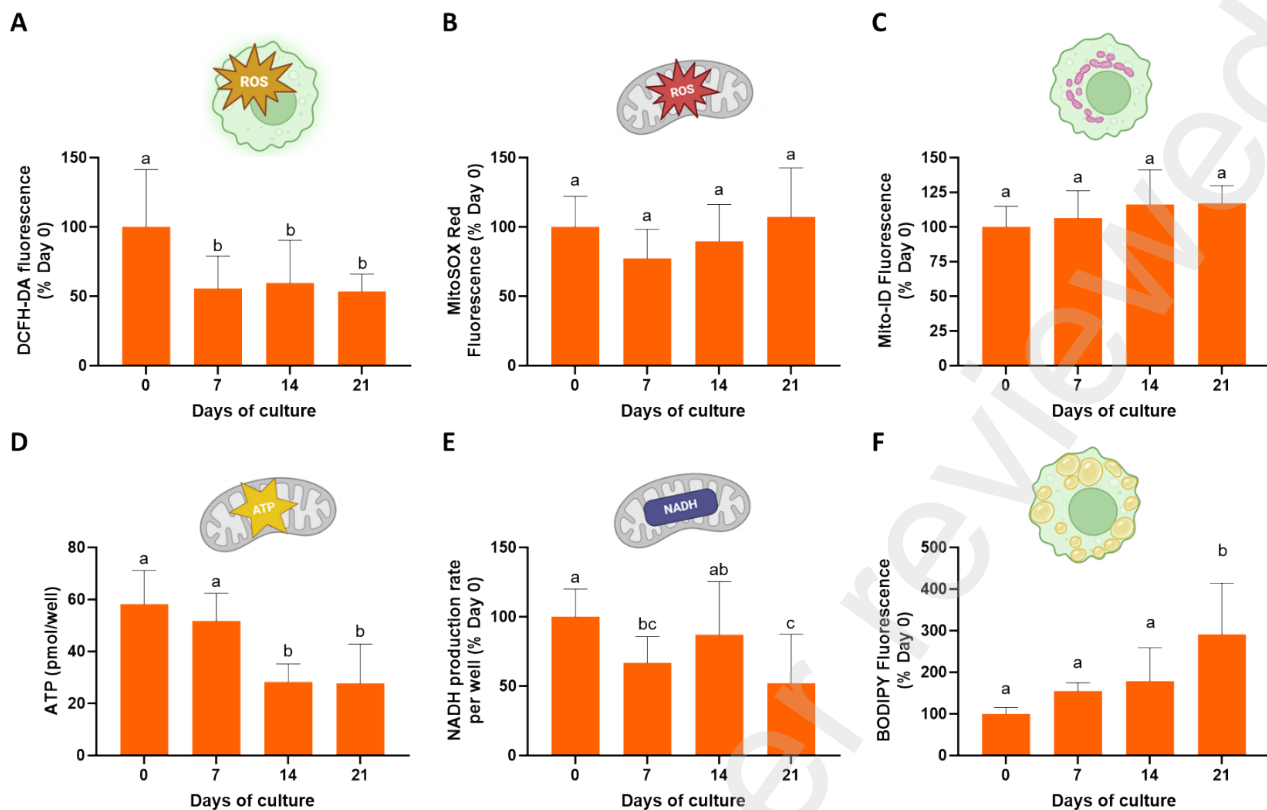
363 *Figure 6.* Viability and immune function of *Crassostrea gigas* hemocytes in primary cultures over time. Cells were cultivated with filtered-
364 sterile oyster's blood plasma with antibiotics (FSOP+PS) in 24-well plates. Day 0 corresponds to cells freshly collected from oysters and not
365 placed in culture. (A) cell viability, (B) the percentage of cells capable of engulfing polystyrene beads, and (C) the average number of
366 polystyrene beads engulfed per cell. Bars represent means \pm standard deviation. Different letters mean significant differences between groups.
367 Results were considered significantly different when $p < 0.05$.

368

369 3.7 Hemocytes present in the long-term primary cultures display some metabolic changes to the *in vitro* 370 environment

371 Additional assays were conducted over time to determine the overall physiological state of the hemocytes in primary
372 cultures. Quantification of basal ROS production, measured through DCFH-DA staining, revealed that cells in culture
373 under all timepoints presented lower intracellular ROS levels than fresh hemolymph samples (Fig. 7A). On the other
374 hand, analysis of mitochondrial superoxide production using the MitoSOX Red staining did not indicate changes on
375 mitochondrial ROS production overtime (Fig. 7B). No changes were also detected in mitochondrial content, measured
376 by the MitolID Green staining (Fig. 7C). It is important to highlight that these three parameters were analyzed by flow
377 cytometry and were calculated as average signal per cell. Additional analyses of mitochondrial parameters by
378 luminescence and fluorescence spectroscopy indicated lower ATP levels after 14 and 21 days (Fig. 7D) as well as
379 lower NADH production rates after 7 and 21 days (Fig. 7E). Contrary to the assays with flow cytometry, these
380 parameters were measured as the average luminescence or fluorescence signal per well. Finally, flow cytometry
381 analysis of the neutral lipid reserve content within each cell revealed a time-dependent higher accumulation, reaching
382 statistically significant values within cells from the day 21 cultures (Fig. 7F).

383



385 *Figure 7.* Metabolism-related parameters of *Crassostrea gigas* hemocytes in primary culture over time. Cells were cultivated with filtered-sterile
 386 oyster's blood plasma with antibiotics (FSOP+PS) in 24-well or 96-well plates and harvested at the specified days of culture. Day 0 corresponds
 387 to cells freshly collected from oysters and not placed in culture. Flow cytometry analyses were made to quantify (A) basal ROS production, (B)
 388 mitochondrial ROS production (C) mitochondrial content, and (F) lipid reserves per cell. Plate reader assays were conducted to quantify (D)
 389 ATP and (E) NADH production per well. Bars represent means \pm standard deviation. Different letters mean significant differences between
 390 groups. Results were considered significantly different when $p < 0.05$.

392 4. Discussion

393 Despite attempts dating back to the 1960s, at present, primary cultures are the only approach for culturing mollusk
 394 cells as not a single marine mollusk cell line is available [31]. Researchers have been developing primary culture
 395 systems for bivalves since the mid-1900s, which led to the initial establishment of oyster heart and mantle tissue cell
 396 cultures [32]. Even though such cell types can be cultured for several weeks, hemocytes are still bivalves most used
 397 primary cells, since they are key indicators of organism physiological and immune status [33,34]. Bivalve hemocytes
 398 have been the subject of great interest in biology and environmental sciences due to their crucial role in immune
 399 defense and maintenance of bivalve health. The diverse functions of bivalve hemocytes encompass a wide range of
 400 biological processes, including pathogen recognition, phagocytosis, immune signaling, encapsulation, tissue repair,
 401 detoxification, nutrient transport, wound healing, ion regulation, and waste clearance [2,35,36]. Indeed, the study of
 402 bivalve hemocyte biology is an area of active research that holds great promise for advancing our understanding of
 403 animal immune function, metabolic regulation, stress responses, and ecotoxicology. Given the significance of marine
 404 bivalve aquaculture to the global economy and prevailing disease threats, the need for a marine bivalve immune cell
 405 culture tool is critical. However, until now, researchers have relied mostly on short-term cultures, limiting their
 406 applicability in research.

407 Moreover, the literature related a huge diversity in the culture conditions of hemocytes. A recent study reviewed the
 408 conditions for primary cell culture of hemocytes from the mussels *Mytilus edulis* and *Mytilus galloprovincialis* [26].
 409 The protocols mentioned by the review were developed to be applied in 24 or 96-well plates at cellular densities similar
 410 to the ones proposed in this study ($2 - 10 \times 10^5$ cells/ml). The main difference was the use of anti-aggregation solution

411 (containing EDTA), commercial culture media (Eagle's Basal Medium or Leibovitz L-15) adjusted to an osmolality of
412 990 – 1050 mOSM/kg, and supplementation with fetal bovine serum or glucose. Studies with *C. gigas* hemocytes also
413 commonly use L-15 medium [33,37] or 0.22 μ m filtered seawater [19,38]. In such circumstances, hemocytes can
414 typically survive for 2-4 days when cultured [26]. It is important to note that Eagle's Basal Medium and L-15 medium
415 do not contain certain amino acids like proline and taurine found in high concentrations in oyster hemolymph [39]. In
416 addition, traditional cell culture media are developed to saturate cell culture with the necessary nutrients to maintain
417 stable and maximal proliferation of cancer cells [40], which is not the case for hemocyte primary cultures. Such balance
418 between antibiotic supplementation and culture medium components is critical to ensure hemocyte health and
419 immunological function during primary culture conditions. Our hemocyte culture approach differs from other studies
420 as we use hemolymph plasma as a natural cellular culture medium. This approach mimics the hemocyte's natural
421 microenvironment, thus providing the cells with a context that is closer to their *in vivo* conditions. This method allows
422 the maintenance of viable and functional *C. gigas* hemocytes for 21 days and even beyond in some cases, while many
423 studies with bivalves detect a loss of viability before 2-7 days of culture [26,34]. Indeed, the use of a plasma-like cell
424 culture medium has also recently been adopted for mammalian cell culture, based on increasing evidence that artificial
425 cell media can largely interfere with cellular processes and metabolism [40]. Hemolymph plasma also contains immune
426 system components such as neurotransmitters, opsonins, hormones, and LPS-binding proteins [41,42], making it an
427 ideal cellular medium for studies on immune responses, inflammation, and host-microbe interactions. Nonetheless,
428 one major disadvantage of this approach is the lack of a standardized cell culture medium. Indeed, oyster plasma
429 composition can vary among individuals and environmental factors [43,44], thus possibly introducing differences in
430 cellular responses to abiotic and biotic factors. For example, different plasma compositions could impact the
431 characterization of the cytotoxicity risk of pollutants. To minimize this drawback, we adopted the strategy of creating
432 a big *C. gigas* plasma bank to be used throughout a same set of experiments. Our success in culturing *C. gigas*
433 hemocytes using plasma can now foster future studies focusing on a thorough characterization of oyster plasma organic
434 and inorganic composition to support the creation of a plasma-like standardized culture medium for oyster cells.

435 Live-cell imaging has become an invaluable technique in cell biology, allowing researchers to observe dynamic
436 processes in living cells in real-time. In the study of bivalve hemocytes, live-cell imaging offers crucial insights into
437 the cellular and molecular mechanisms underlying immune responses, environmental stress adaptations, and disease
438 resistance. In this study, we adopted live-cell imaging techniques to monitor hemocyte primary cultures over time.
439 This non-invasive, label-free approach allowed us to easily screen between the different cell culture conditions during
440 the primary culture optimization phase to determine if hemocytes were alive based on their motility behavior.
441 Moreover, by combining such a technique with MGG staining, we were able to determine that some morphotypes
442 corresponded to different movement states of the cells. From such observations, we suggest that fresh hemolymph
443 samples are composed of at least 5 distinct hemocyte types: blast-like cells, two small highly mobile cell types with
444 and without granules (dendritic-like cells), and two less mobile cell types without granules (fibroblast-like cells) and
445 with granules (macrophage-like cells). Such findings differ from what most publications describe regarding the
446 diversity of *C. gigas* hemocyte subpopulations, which report mainly three hemocyte types: blast-like cells,
447 hyalinocytes, and granulocytes [2]. We believe this distinction is because most studies usually analyze fixed hemocyte
448 samples, while in our study hemocytes are alive and, therefore free to acquire different shapes. Such an approach has
449 the advantage of offering additional support in understanding the role of each morphotype. For example, large
450 hyalinocytes that appeared highly spread and adhered to the cell culture plate (fibroblast-like cells) might have a
451 function of aggregation and wound healing, as seen for other bivalve species [2]. Our live-cell imaging of hemocytes
452 together with microbeads strengthens this hypothesis, as these fibroblast-like cells did not display any phagocytic
453 capacity. Our study, therefore, underlines the need to further investigate the function of the different types of hemocytes
454 to help understand their respective role *in vivo* and the need to get a more comprehensive and unified characterization
455 of these different types of hemocytes. Our primary cultures maintained the above-mentioned hemocyte variety of at
456 least 5 different hemocyte types for 7 days. Cell diversity loss became more evident after 14 and 21 days, with a
457 noticeable decrease in the proportion of blast-like cells and fibroblast-like cells, and an enrichment of more complex
458 cells. Thus, we hypothesize granulocytes represent a more resistant hemocyte subpopulation to our *in vitro* conditions.
459 Interestingly, the surviving subpopulations present at later culture periods, rather than exhibiting symptoms of aging
460 and functional loss, exhibited stable immunological function as measured by phagocytic competence.

461 Phagocytosis is a crucial marker of immune function in hemocytes [45]. Our protocol shows no loss of hemocyte
462 phagocytic activity and capacity over 21 days of culture. Moreover, we observed that the phagocytosis capacity
463 (number of beads phagocytosed per cell) increased at 21 days of culture. This increase correlates with the significant
464 changes in hemocyte morphotypes present in culture at this time point. Indeed, we found a decrease in the abundance
465 of non-phagocytic cell types such as the fibroblast-like hyalinocytes, and an enrichment of larger and more complex
466 hemocytes. It is worth noting that more complex cells, such as granulocytes, are bivalves' most active phagocytic
467 immune cells [46]. Thus, even if we note a noticeable loss of diversity within our 21-day cultures, it is likely that they
468 were enriched with phagocyte cells, opening interesting avenues for bivalve immune system research and longer-term
469 effects of environmental factors on immune capacity.

470 To further understand the physiology of our hemocyte primary cultures we analyzed key metabolic parameters to
471 investigate possible metabolic alterations and reprogramming in response to the altered microenvironmental settings.
472 ROS production is closely related to cellular metabolic activity. Indeed, mitochondrial ROS is the major contributor
473 to ROS levels in *C. gigas* hemocytes [47]. In this study, we have shown that total basal ROS production is higher in
474 fresh hemocytes on day 0, then becomes lower and stable until day 21 cultures. Recently, we have found that, in *C.*
475 *gigas*, the average physiological oxygen level within oyster hemolymph is ~5 kPa, but it can vary between 0 kPa and
476 12 kPa depending on valve opening behavior and filtering activities [22]. However, ambient air is composed of 21 kPa
477 O₂. Thus, when hemocytes are transferred from the *in vivo* to *in vitro* conditions, they are exposed to much higher
478 levels of oxygen than they would naturally experience (hyperoxia). Indeed, ROS production in cells is known to
479 increase at hyperoxia conditions [48,49], which could explain the high ROS levels in the fresh hemocytes (day 0). The
480 subsequent decrease and stabilization of ROS production at the following periods of culture (Days 7, 14, and 21) can
481 be due to hemocyte acclimation mechanisms. We hypothesize that such mechanisms may be mediated by the activation
482 of the nuclear factor erythroid 2-related factor 2 (Nrf2) transcription factor which is a master regulator of antioxidant
483 cellular responses [22]. This hypothesis is supported by the fact that the conserved role of Nrf2 in mediating redox
484 changes was already confirmed in *C. gigas* [22,50,51], and that Nrf2 activation in cells submitted to hyperoxia
485 condition (ambient air) is a well-described phenomenon within mammalian cell culture models [52]. Future studies
486 performing gene expression analyses of Nrf2-target genes over the course of the hemocyte primary cultures should be
487 performed to confirm this hypothesis.

488 However, throughout the 21 days of culture, we found stable levels of mitochondrial ROS, which can be a proxy for
489 mitochondrial activity [53]. At first glance, this result seems to contradict our first hypothesis related to the Nrf2-
490 mediated adaptive mechanisms of hemocytes in culture. Nonetheless, the differences reported between the total basal
491 ROS and mitochondrial ROS can be related to differences in probe specificities. DCF is a broader marker of ROS,
492 reacting with several different ROS types, whereas MitoSOX is a marker specific for superoxide anion related to
493 mitochondrial activity, membrane potential, and size [54]. Moreover, the analysis of hemocyte mitochondrial content
494 remained constant throughout the cell culture period. Cellular stress and mitochondrial dysfunction usually alter
495 mitochondrial dynamics, often leading to changes in mitochondrial content through mitophagy or biogenesis
496 mechanisms, for example [55]. Since this was not the case in our study, our primary hemocyte culture model offers
497 stable conditions to study mitochondrial dynamics under different stress and disease scenarios.

498 Meanwhile, the total ATP levels detected in each well decreased at 7 days of culture and then stabilized at lower levels
499 throughout the culture until 21 days. Additionally, the rate of total NADH production per well, which is also indicative
500 of mitochondrial activity, was lower at days 7 and 21 of culture. We hypothesize that such lower levels are not
501 necessarily a slowdown in the cellular metabolism, but rather indicative of cell death and/or loss over the 21-day culture
502 period, leading to a decrease in the total cellular content per well. To better elucidate this hypothesis, future studies
503 can be performed using high-content imaging and automated analysis of cellular content for a better normalization of
504 the metabolic activity per cell, as soon as such tools become more available and adaptable to marine cell cultures.

505 Lipid droplets act as dynamic organelles for storing neutral lipids and play a crucial role in energy homeostasis and
506 lipid metabolism. They are involved in various cellular processes, including the regulation of lipid synthesis and
507 degradation, signaling pathways, and the maintenance of cellular lipid balance [56]. We have identified changes in
508 intracellular dynamics of neutral lipid storage in hemocytes, leading to higher lipid accumulation at 21 days of cell
509 culture. Lipid accumulation in cultured cells can be a sign of changes in lipid metabolism, or the ability to take up

lipids from the media, or as a result of autophagic processes [57]. Indeed, to interpret our result, there are at least three critical points to consider. Firstly, in bivalves, hemocytes are known to transport nutrients, including lipids, by absorbing them from the alimentary tract and transferring them to other tissues or developing oocytes [58,59]. Secondly, granulocytes, which were enriched at the 21-day cultures, have a higher neutral lipid content than other cell types in marine bivalves [60]. Thirdly, reserves of neutral lipids are related to the balance between synthesis and degradation in response to metabolic needs and shifts. Thus, it is likely that the absence of interaction between hemocytes and other tissues in the cultures blocked their ability to transport lipids to other cells, promoting a higher accumulation of lipids absorbed through the cell culture medium (FSOP). This higher neutral lipid accumulation could be related to the larger cell size observed after 21 days of culture. Taken together, the higher levels of neutral lipids in hemocytes in the second and third week of cell culture are possibly related to cellular size, composition, and energy allocation changes.

As discussed above, our results suggest potential changes in cellular metabolism over 21 days of culture. This presents a limitation when studying the biology of hemocytes in extended culture periods. However, it adds important information on the implications of cell microenvironment conditions to the success and function of bivalve primary hemocyte cultures. The established protocol presented here opens new avenues to explore biotic and abiotic conditions that can further improve hemocyte primary cultures and potentially even develop a cell line if conditions favoring proliferation are found. Moreover, it also provides the possibility to investigate the behavior of cell cultures under different stress conditions. For example, it is possible now to explore whether pathogens, contaminants, temperature, or plasma composition alterations will affect hemocyte viability and function over extended periods. Thus, this standardized long-term hemocyte primary culture, allied with the cell-based assays optimized in this study, allows the investigation of factors that can induce stress responses affecting cellular morphology, behavior, viability, immunocompetence, mitochondrial metabolism, and lipid storage. This could lead to new insights and discoveries in hemocyte biology and ecotoxicology research, thus expanding our understanding of bivalves' immunological and metabolic responses to the current and future challenges of our changing ocean.

5. Concluding remarks

In conclusion, our study of bivalve hemocytes in primary culture has provided valuable insights into their immunological competence, metabolic responses, and cellular behavior over an extended 21-day period. Bivalve hemocytes, known for their critical roles in immune defense and overall health, present a versatile model for studying various biological processes. Utilizing hemolymph plasma as a natural cellular culture medium, our approach offers a context approaching *in vivo* conditions. This method demonstrated sustained hemocyte phagocytic activity and capacity over the 21-day culture, highlighting the robustness of bivalve hemocytes in this unique culture medium. Notably, the increase in phagocytic capacity after 21 days was associated with shifts in hemocyte populations, indicating a dynamic response to prolonged culture conditions. We also revealed significant insights into the metabolic adaptation of hemocytes to *in vitro* conditions. Lastly, this proposed primary hemocyte culture protocol employs diverse health, function, and metabolic markers, presenting a valuable resource for *in vitro* research with hemocytes. The application of our protocols to different bivalve species holds promise for expanding our understanding of their immunological and metabolic responses in the face of ongoing and future challenges in our changing oceans. This can significantly support the ever-growing need for further hemocyte, immunology, and ecotoxicology research investigations.

6. References

- [1] T.P. Yoshino, U. Bickham, C.J. Bayne, Molluscan cells in culture: primary cell cultures and cell lines., *Can J Zool* 91 (2013). <https://doi.org/10.1139/cjz-2012-0258>.
- [2] N.R. de la Ballina, F. Maresca, A. Cao, A. Villalba, Bivalve Haemocyte Subpopulations: A Review, *Front Immunol* 13 (2022) 826255. <https://doi.org/10.3389/FIMMU.2022.826255/BIBTEX>.

- 556 [3] L. Song, L. Wang, L. Qiu, Z. Huan, Bivalve immunity, in: K. Söderhäll (Ed.), *Invertebrate Immunity*, Landes
557 Bioscience and Springer Science+Business Media, New York, 2010: pp. 44–65.
- 558 [4] B.L. Bayne, M.N. Moore, J. Widdows, D.R. Livingstone, P. Salkeld, Measurement of the responses of
559 individuals to environmental stress and pollution: studies with bivalve molluscs, *Philosophical Transactions of the*
560 *Royal Society of London. B, Biological Sciences* 286 (1979) 563–581. <https://doi.org/10.1098/RSTB.1979.0046>.
- 561 [5] R.K. Pipe, J.A. Coles, Environmental contaminants influencing immunefunction in marine bivalve molluscs,
562 *Fish Shellfish Immunol* 5 (1995) 581–595. [https://doi.org/10.1016/S1050-4648\(95\)80043-3](https://doi.org/10.1016/S1050-4648(95)80043-3).
- 563 [6] T. Renault, Immunotoxicological effects of environmental contaminants on marine bivalves, *Fish Shellfish*
564 *Immunol* 46 (2015) 88–93. <https://doi.org/10.1016/J.FSI.2015.04.011>.
- 565 [7] M. Auffret, Bivalves as Models for Marine Immunotoxicology, in: *Investigative Immunotoxicology*, CRC
566 Press, 2005: pp. 49–68. <https://doi.org/10.1201/9781420036817-8>.
- 567 [8] M. Abdou, L. Dutruch, J. Schäfer, B. Zaldibar, R. Medrano, U. Izagirre, T. Gil-Díaz, C. Bossy, C. Catrouillet,
568 R. Hu, A. Coynel, A. Lerat, A. Cobelo-García, G. Blanc, M. Soto, Tracing platinum accumulation kinetics in oyster
569 *Crassostrea gigas*, a sentinel species in coastal marine environments, *Science of The Total Environment* 615 (2018)
570 652–663. <https://doi.org/10.1016/J.SCITOTENV.2017.09.078>.
- 571 [9] E. David, A. Tanguy, R. Riso, L. Quiniou, J. Laroche, D. Moraga, Responses of Pacific oyster *Crassostrea*
572 *gigas* populations to abiotic stress in environmentally contrasted estuaries along the Atlantic coast of France, *Aquatic*
573 *Toxicology* 109 (2012) 70–79. <https://doi.org/10.1016/J.AQUATOX.2011.11.014>.
- 574 [10] D.F. Mello, R. Trevisan, N.M. Danielli, A.L. Dafre, Vulnerability of glutathione-depleted *Crassostrea gigas*
575 oysters to *Vibrio* species, *Mar Environ Res* 154 (2020) 104870. <https://doi.org/10.1016/j.marenvres.2019.104870>.
- 576 [11] L. Nogueira, D.F. Mello, R. Trevisan, D. Garcia, D. da Silva Acosta, A.L. Dafre, E.A. de Almeida, Hypoxia
577 effects on oxidative stress and immunocompetence biomarkers in the mussel *Perna perna* (Mytilidae, Bivalvia), *Mar*
578 *Environ Res* 126 (2017) 109–115. <https://doi.org/10.1016/j.marenvres.2017.02.009>.
- 579 [12] R. Trevisan, D.F. Mello, M. Uliano-Silva, G. Delapiedra, M. Arl, A.L. Dafre, The biological importance of
580 glutathione peroxidase and peroxiredoxin backup systems in bivalves during peroxide exposure, *Mar Environ Res* 101
581 (2014) 81–90. <https://doi.org/10.1016/j.marenvres.2014.09.004>.
- 582 [13] R. Trevisan, M. Arl, C.L. Sacchet, C.S. Engel, N.M. Danielli, D.F. Mello, C. Brocardo, A.F. Maris, A.L. Dafre,
583 Antioxidant deficit in gills of Pacific oyster (*Crassostrea gigas*) exposed to chlorodinitrobenzene increases menadione
584 toxicity, *Aquatic Toxicology* 108 (2012). <https://doi.org/10.1016/j.aquatox.2011.09.023>.
- 585 [14] R. Trevisan, G. Delapiedra, D.F. Mello, M. Arl, É.C. Schmidt, F. Meder, M. Monopoli, E. Cargin-Ferreira,
586 Z.L. Bouzon, A.S. Fisher, D. Sheehan, A.L. Dafre, Gills are an initial target of zinc oxide nanoparticles in oysters
587 *Crassostrea gigas*, leading to mitochondrial disruption and oxidative stress, *Aquatic Toxicology* 153 (2014) 27–38.
588 <https://doi.org/10.1016/j.aquatox.2014.03.018>.
- 589 [15] D.F. Mello, L.A. de O. Proença, M.A. Barracco, Comparative Study of Various Immune Parameters in Three
590 Bivalve Species during a Natural Bloom of *Dinophysis acuminata* in Santa Catarina Island, Brazil, *Toxins (Basel)* 2
591 (2010) 1166–1178. <https://doi.org/10.3390/toxins2051166>.
- 592 [16] M. Auffret, N. Mujdzic, C. Corporeau, D. Moraga, Xenobiotic-induced immunomodulation in the European
593 flat oyster, *Ostrea edulis*, *Mar Environ Res* 54 (2002) 585–589. [https://doi.org/10.1016/S0141-1136\(02\)00120-4](https://doi.org/10.1016/S0141-1136(02)00120-4).
- 594 [17] N. Weng, J. Meng, S. Huo, F. Wu, W.X. Wang, Hemocytes of bivalve mollusks as cellular models in
595 toxicological studies of metals and metal-based nanomaterials, *Environmental Pollution* 312 (2022) 120082.
596 <https://doi.org/10.1016/J.ENVPOL.2022.120082>.

- 597 [18] A. Katsumiti, A.J. Thorley, I. Arostegui, P. Reip, E. Valsami-Jones, T.D. Tetley, M.P. Cajaraville, Cytotoxicity
598 and cellular mechanisms of toxicity of CuO NPs in mussel cells in vitro and comparative sensitivity with human cells,
599 *Toxicology in Vitro* 48 (2018) 146–158. <https://doi.org/10.1016/J.TIV.2018.01.013>.
- 600 [19] D.F. Mello, E.S. De Oliveira, R.C. Vieira, E. Simoes, R. Trevisan, A.L. Dafre, M.A. Barracco, Cellular and
601 Transcriptional Responses of *Crassostrea gigas* Hemocytes Exposed in Vitro to Brevetoxin (PbTx-2), *Marine Drugs*
602 2012, Vol. 10, Pages 583-597 10 (2012) 583–597. <https://doi.org/10.3390/MD10030583>.
- 603 [20] D.F. Mello, M. Arl, R. Trevisan, A.L. Dafre, How important are glutathione and thiol reductases to oyster
604 hemocyte function?, *Fish Shellfish Immunol* 46 (2015) 566–72. <https://doi.org/10.1016/j.fsi.2015.07.017>.
- 605 [21] J.R. Meadows, J.C. DeWitt, A.A. Rooney, Ecoimmunotoxicology-An Overview, in: *Comprehensive*
606 *Toxicology: Third Edition*, Elsevier, 2018: pp. 886–891. <https://doi.org/10.1016/B978-0-12-801238-3.64244-7>.
- 607 [22] R. Trevisan, D.F. Mello, Redox control of antioxidants, metabolism, immunity, and development at the core
608 of stress adaptation of the oyster *Crassostrea gigas* to the dynamic intertidal environment, *Free Radic Biol Med* 210
609 (2024) 85–106. <https://doi.org/10.1016/J.FREERADBIOMED.2023.11.003>.
- 610 [23] L. Donaghy, A.K. Volety, Functional and metabolic characterization of hemocytes of the green mussel, *Perna*
611 *viridis*: in vitro impacts of temperature, *Fish Shellfish Immunol* 31 (2011) 808–814.
612 <https://doi.org/10.1016/J.FSI.2011.07.018>.
- 613 [24] P. Moreau, T. Burgeot, T. Renault, Pacific oyster (*Crassostrea gigas*) hemocyte are not affected by a mixture
614 of pesticides in short-term in vitro assays, *Environmental Science and Pollution Research* 21 (2014) 4940–4949.
615 <https://doi.org/10.1007/S11356-013-1931-3/METRICS>.
- 616 [25] C. Roman, P. Mahé, O. Latchere, C. Catrouillet, J. Gigault, I. Métais, A. Châtel, Effect of size continuum from
617 nanoplastics to microplastics on marine mussel *Mytilus edulis*: Comparison in vitro/in vivo exposure scenarios,
618 *Comparative Biochemistry and Physiology Part C: Toxicology & Pharmacology* 264 (2023) 109512.
619 <https://doi.org/10.1016/J.CBPC.2022.109512>.
- 620 [26] A. Barrick, C. Guillet, C. Mouneyrac, A. Châtel, Investigating the establishment of primary cultures of
621 hemocytes from *Mytilus edulis*, *Cytotechnology* 70 (2018) 1205–1220. <https://doi.org/10.1007/S10616-018-0212-X/METRICS>.
- 622
- 623 [27] B. Petton, D. Destoumieux-Garzón, F. Pernet, E. Toulza, J. de Lorgeril, L. Degremont, G. Mitta, The Pacific
624 Oyster Mortality Syndrome, a Polymicrobial and Multifactorial Disease: State of Knowledge and Future Directions,
625 *Front Immunol* 0 (2021) 52. <https://doi.org/10.3389/FIMMU.2021.630343>.
- 626 [28] M. Delaporte, P. Soudant, J. Moal, E. Giudicelli, C. Lambert, C. Séguineau, J.F. Samain, Impact of 20:4n-6
627 supplementation on the fatty acid composition and hemocyte parameters of the pacific oyster *crassostrea gigas*, *Lipids*
628 41 (2006) 567–576. <https://doi.org/10.1007/S11745-006-5006-9>.
- 629 [29] C. Lambert, P. Soudant, G. Choquet, C. Paillard, Measurement of *Crassostrea gigas* hemocyte oxidative
630 metabolism by flow cytometry and the inhibiting capacity of pathogenic vibrios, *Fish Shellfish Immunol* 15 (2003)
631 225–240. [https://doi.org/10.1016/S1050-4648\(02\)00160-2](https://doi.org/10.1016/S1050-4648(02)00160-2).
- 632 [30] M. Delaporte, P. Soudant, J. Moal, C. Lambert, C. Quéré, P. Miner, G. Choquet, C. Paillard, J.F. Samain,
633 Effect of a mono-specific algal diet on immune functions in two bivalve species - *Crassostrea gigas* and *Ruditapes*
634 *philippinarum*, *Journal of Experimental Biology* 206 (2003) 3053–3064. <https://doi.org/10.1242/JEB.00518>.
- 635 [31] S. Balakrishnan, I.S.B. Singh, J. Puthumana, Status in molluscan cell line development in last one decade
636 (2010–2020): impediments and way forward, *Cytotechnology* 74 (2022) 433. <https://doi.org/10.1007/S10616-022-00539-X>.
- 637
- 638 [32] E. Mialhe, V. Boulo, H. Grizel, Bivalve Mollusc Cell Culture, *American Fisheries Society Special Publication*
639 18 (1988) 311–315.

- 640 [33] R.W.A. Potts, A.P. Gutierrez, Y. Cortés-Araya, R.D. Houston, T.P. Bean, Developments in marine
641 invertebrate primary culture reveal novel cell morphologies in the model bivalve *Crassostrea gigas*, *PeerJ* 2020 (2020)
642 e9180. <https://doi.org/10.7717/PEERJ.9180/SUPP-15>.
- 643 [34] R. Ladhar-Chaabouni, A. Hamza-Chaffai, The cell cultures and the use of haemocytes from marine molluscs
644 for ecotoxicology assessment, *Cytotechnology* 68 (2016) 1669. <https://doi.org/10.1007/S10616-015-9932-3>.
- 645 [35] Y. Labreuche, C. Lambert, P. Soudant, V. Boulo, A. Huvet, J.L. Nicolas, Cellular and molecular hemocyte
646 responses of the Pacific oyster, *Crassostrea gigas*, following bacterial infection with *Vibrio aestuarianus* strain 01/32,
647 *Microbes Infect* 8 (2006) 2715–2724. <https://doi.org/10.1016/J.MICINF.2006.07.020>.
- 648 [36] W.S. Fisher, Structure and Functions of Oyster Hemocytes, (1986) 25–35. https://doi.org/10.1007/978-3-642-70768-1_3.
- 650 [37] W. Wang, M. Li, L. Wang, H. Chen, Z. Liu, Z. Jia, L. Qiu, L. Song, The granulocytes are the main
651 immunocompetent hemocytes in *Crassostrea gigas*, *Dev Comp Immunol* 67 (2017) 221–228.
652 <https://doi.org/10.1016/J.DCI.2016.09.017>.
- 653 [38] B. Gagnaire, H. Thomas-Guyon, T. Burgeot, T. Renault, Pollutant effects on Pacific oyster, *Crassostrea gigas*
654 (Thunberg), hemocytes: Screening of 23 molecules using flow cytometry, *Cell Biol Toxicol* 22 (2006) 1–14.
655 <https://doi.org/10.1007/S10565-006-0011-6/METRICS>.
- 656 [39] S.N. Chen, C.M. Wen, Establishment of cell lines derived from oyster, *Crassostrea gigas* Thunberg and hard
657 clam, *Meretrix lusoria* Roding, *Methods in Cell Science* 21 (1999) 183–192.
658 <https://doi.org/10.1023/A:1009829807954/METRICS>.
- 659 [40] M. V. Golikov, V.T. Valuev-Elliston, O.A. Smirnova, A. V. Ivanov, Physiological Media in Studies of Cell
660 Metabolism, *Mol Biol* 56 (2022) 629–637. <https://doi.org/10.1134/S0026893322050077/METRICS>.
- 661 [41] P. Schmitt, R.D. Rosa, M. Duperthuy, J. de Lorgeril, E. Bachère, D. Destoumieux-Garzón, The antimicrobial
662 defense of the Pacific oyster, *Crassostrea gigas*. How diversity may compensate for scarcity in the regulation of
663 resident/pathogenic microflora, *Front Microbiol* 3 (2012) 23326.
664 <https://doi.org/10.3389/FMICB.2012.00160/BIBTEX>.
- 665 [42] Z. Liu, L. Wang, Z. Zhou, Y. Sun, M. Wang, H. Wang, Z. Hou, D. Gao, Q. Gao, L. Song, The simple
666 neuroendocrine-immune regulatory network in oyster *Crassostrea gigas* mediates complex functions, *Scientific*
667 *Reports* 2016 6:1 6 (2016) 1–13. <https://doi.org/10.1038/srep26396>.
- 668 [43] N. Itoh, Q.G. Xue, K.L. Schey, Y. Li, R.K. Cooper, J.F. La Peyre, Characterization of the major plasma protein
669 of the eastern oyster, *Crassostrea virginica*, and a proposed role in host defense, *Comp Biochem Physiol B Biochem*
670 *Mol Biol* 158 (2011) 9–22. <https://doi.org/10.1016/J.CBPB.2010.06.006>.
- 671 [44] H.C. Song, C.Y. Xie, Q. Kong, L. Wei, X.T. Wang, Daylight ultraviolet B radiation ruptured the cell
672 membrane, promoted nucleotide metabolism and inhibited energy metabolism in the plasma of Pacific oyster, *Sci Total*
673 *Environ* 862 (2023). <https://doi.org/10.1016/J.SCITOTENV.2022.160729>.
- 674 [45] L. Wang, X. Song, L. Song, The oyster immunity, *Dev Comp Immunol* 80 (2018) 99–118.
675 <https://doi.org/10.1016/J.DCI.2017.05.025>.
- 676 [46] S. Jiang, Z. Jia, T. Zhang, L. Wang, L. Qiu, J. Sun, L. Song, Functional characterisation of phagocytes in the
677 Pacific oyster *Crassostrea gigas*, *PeerJ* 2016 (2016) e2590. <https://doi.org/10.7717/PEERJ.2590/SUPP-1>.
- 678 [47] L. Donaghy, E. Kraffe, N. Le Goïc, C. Lambert, A.K. Volety, P. Soudant, Reactive oxygen species in
679 unstimulated hemocytes of the pacific oyster *Crassostrea gigas*: a mitochondrial involvement., *PLoS One* 7 (2012)
680 e46594. <https://doi.org/10.1371/journal.pone.0046594>.

- 681 [48] L. Donaghy, S. Artigaud, R. Sussarellu, C. Lambert, N. Le Goïc, H. Hégaret, P. Soudant, Tolerance of bivalve
682 mollusc hemocytes to variable oxygen availability: a mitochondrial origin?, *Aquat Living Resour* 26 (2013) 257–261.
683 <https://doi.org/10.1051/ALR/2013054>.
- 684 [49] D.L. Hoffman, P.S. Brookes, Oxygen sensitivity of mitochondrial reactive oxygen species generation depends
685 on metabolic conditions, *Journal of Biological Chemistry* 284 (2009) 16236–16245.
686 <https://doi.org/10.1074/jbc.M809512200>.
- 687 [50] N.M. Danielli, R. Trevisan, D.F. Mello, K. Fischer, V.S. Deconto, D. da Silva Acosta, A. Bianchini, A.C.D.
688 Bainy, A.L. Dafre, Upregulating Nrf2-dependent antioxidant defenses in Pacific oysters *Crassostrea gigas*:
689 Investigating the Nrf2/Keap1 pathway in bivalves, *Comparative Biochemistry and Physiology Part C: Toxicology &*
690 *Pharmacology* 195 (2017) 16–26. <https://doi.org/10.1016/J.CBPC.2017.02.004>.
- 691 [51] N.M. Danielli, R. Trevisan, D.F. Mello, K. Fischer, V.S. Deconto, A. Bianchini, A.C.D. Bainy, A.L. Dafre,
692 Contrasting effects of a classic Nrf2 activator, tert-butylhydroquinone, on the glutathione-related antioxidant defenses
693 in Pacific oysters, *Crassostrea gigas*, *Mar Environ Res* 130 (2017) 142–149.
694 <https://doi.org/10.1016/J.MARENRES.2017.07.020>.
- 695 [52] D.C.J. Ferguson, G.R. Smerdon, L.W. Harries, N.J.F. Dodd, M.P. Murphy, A. Curnow, Altered cellular redox
696 homeostasis and redox responses under standard oxygen cell culture conditions versus physioxia, *Free Rad Biol Med*
697 126 (2018) 322–333. <https://doi.org/10.1016/j.freeradbiomed.2018.08.025>
- 698 Winyard, Paul G. D.F. Mello, C. Bergemann, K. Fisher, R. Chitrakar, S. Bijwadia, Y. Wang, A. Caldwell, L.R. Baugh,
699 J.N. Meyer, Rotenone modulates *C. elegans* immunometabolism and pathogen susceptibility., *Front Immunol* (2022).
700 <https://doi.org/10.3389/fimmu.2022.840272>.
- 701 [53] B.M. Polster, D.G. Nicholls, S.X. Ge, B.A. Roelofs, Use of Potentiometric Fluorophores in the Measurement
702 of Mitochondrial Reactive Oxygen Species, *Methods Enzymol* 547 (2014) 225–250. <https://doi.org/10.1016/B978-0-12-801415-8.00013-8>.
- 704 [54] M.P. Murphy, H. Bayir, V. Belousov, C.J. Chang, K.J.A. Davies, M.J. Davies, T.P. Dick, T. Finkel, H.J.
705 Forman, Y. Janssen-Heininger, D. Gems, V.E. Kagan, B. Kalyanaraman, N.G. Larsson, G.L. Milne, T. Nyström, H.E.
706 Poulsen, R. Radi, H. Van Remmen, P.T. Schumacker, P.J. Thornalley, S. Toyokuni, C.C. Winterbourn, H. Yin, B.
707 Halliwell, Guidelines for measuring reactive oxygen species and oxidative damage in cells and in vivo, *Nature*
708 *Metabolism* 2022 4:6 4 (2022) 651–662. <https://doi.org/10.1038/s42255-022-00591-z>.
- 709 [55] D.F. Mello, L.L. Maurer, I.T. Ryde, D.H. Song, S.M. Marinakos, J.N. Meyer, In vivo effects of silver
710 nanoparticles on development, behavior and mitochondrial function are altered by genetic defects in mitochondrial
711 dynamics, Submitted to *Environmental Science and Technology* (2021).
- 712 [56] T.C. Walther, R. V. Farese, Lipid Droplets And Cellular Lipid Metabolism, *Annu Rev Biochem* 81 (2012)
713 687. <https://doi.org/10.1146/ANNUREV-BIOCHEM-061009-102430>.
- 714 [57] G.B. Gordon, M.A. Barcza, M.E. Bush, Lipid accumulation in hypoxic tissue culture cells, *American Journal*
715 *of Pathology* 88 (1977) 663–678. <http://europepmc.org/articles/PMC2032384> (accessed May 20, 2024).
- 716 [58] P.G. Beninger, M. Le Penec, Scallop Structure and Function, *Developments in Aquaculture and Fisheries*
717 *Science* 40 (2016) 85–159. <https://doi.org/10.1016/B978-0-444-62710-0.00003-1>.
- 718 [59] R.J. Pollero, G. Huca, R.R. Brenner, Role of hemocytes and plasma on lipid transport in the freshwater mollusc
719 *Diplodon delodontus*, *Comp Biochem Physiol A Physiol* 82 (1985) 339–343. [https://doi.org/10.1016/0300-9629\(85\)90865-5](https://doi.org/10.1016/0300-9629(85)90865-5).
- 721 [60] A. Rolton, N.L.C. Ragg, Green-lipped mussel (*Perna canaliculus*) hemocytes: A flow cytometric study of
722 sampling effects, sub-populations and immune-related functions, *Fish Shellfish Immunol* 103 (2020) 181–189.
723 <https://doi.org/10.1016/J.FSI.2020.05.019>.

724 **Funding**

725 The majority of this work was conducted thanks to a Postdoctoral fellowship from the French government (Finistère
726 Appel APRE and Région Bretagne Appel SAD n°2050). Currently, DF Mello as well as R Trevisan, and FR Queiroga
727 are recipients of postdoctoral fellowships through the Bienvenüe Program, co-funded by the European Union's Horizon
728 2020 research and innovation programme under the Marie Skłodowska-Curie grant agreement number 899546, the
729 Region Bretagne, and the Université de Bretagne Occidentale. H Gabe was recipient of a sandwich doctorate
730 scholarship from the Government of Brazil funded by the "Conselho Nacional de Desenvolvimento Científico e
731 Tecnológico – CNPq" (Process Process 200247/2022-0). This work was supported by ISblue project, Interdisciplinary
732 graduate school for the blue planet (ANR-17-EURE-0015) and co-funded by a grant from the French government
733 under the program "Investissements d'Avenir"; embedded in France 2030. This study is set within the framework of
734 the « Laboratoire d'Excellence (LabEx) » TULIP (ANR-10-LABX-41). It was supported by the École Universitaire
735 de Recherche TULIP-GS (ANR-18-EURE-0019).

736

737 **Acknowledgements**

738 The authors would like to thank Christine Dubreuil, Olivier Mouchel, Moussa Diagne, Hugo Koechlin, Luc Lebrun,
739 Nelly Le Goic, and Emma Denmat for their support during the experiments; Philippe Elies for his support to acquire
740 the confocal microscopy images; Claire Hellio for manuscript revision; and Sébastien Herve for the graphical abstract.

741